

Inhibitors of Src Homology-2 Domain Containing Protein Tyrosine Phosphatase-2 (Shp2) Based on Oxindole Scaffolds

Harshani R. Lawrence,^{*,§,†,II} Roberta Pireddu,^{§,†} Liwei Chen,^{†,‡} Yunting Luo,^{†,II} Shen-Shu Sung,^{II} Ann Marie Szymanski,[‡] M. L. Richard Yip,^{II,‡} Wayne C. Guida,^{II,‡,V} Saïd M. Sebti,^{§,‡} Jie Wu,^{§,‡,O} and Nicholas J. Lawrence^{*,§,‡}

Drug Discovery Program, Molecular Oncology Program, and High Throughput Screening and Chemistry Core Facility, Moffitt Cancer Center, 12901 Magnolia Drive, Tampa, Florida 33612, and Departments of Oncologic Sciences, Chemistry, and Molecular Medicine, University of South Florida, Tampa, Florida, 33612

Received March 7, 2008

Screening of the NCI diversity set of compounds has led to the identification of **5** (NSC-117199), which inhibits the protein tyrosine phosphatase (PTP) Shp2 with an IC_{50} of 47 μ M. A focused library incorporating an isatin scaffold was designed and evaluated for inhibition of Shp2 and Shp1 PTP activities. Several compounds were identified that selectively inhibit Shp2 over Shp1 and PTP1B with low to submicromolar activity. A model for the binding of the active compounds is proposed.

Introduction

The function of many proteins, particularly those involved in signal transduction pathways, is dependent upon their tyrosine phosphorylation status, which is finely regulated by the action of protein tyrosine kinases and protein tyrosine phosphatases. Many protein tyrosine kinases such as Bcr-Abl,^a c-kit, ErbB, and VEGFR are validated drug targets for cancer therapy.¹ Less attention has been paid to the development of protein tyrosine phosphatase inhibitors as an alternative strategy to modulate key target protein phosphorylation states.^{2,3} The protein tyrosine phosphatase (PTP) Shp2 is a nonreceptor PTP that plays a positive role in cell signaling by growth factors and cytokines and is involved in regulation of cell proliferation, differentiation, and migration.^{4,5} In particular, Shp2 mediates activation of Erk1 and Erk2 MAP kinases by receptor tyrosine kinases such as ErbB1, ErbB2, and c-Met that are involved in the pathogenesis of human carcinoma.^{6–11} Furthermore, gain-of-function Shp2 mutants are found in childhood hematological malignancies such as juvenile myelomonocytic leukemia, some cases of solid tumors, and are associated with ~50% cases of Noonan syndrome.¹² It has also been reported that Shp2 is a key mediator of the oncogenic CagA protein of *Helicobacter pylori*, which causes gastric cancer.^{13,14} These studies suggest that Shp2 PTP is a molecular target for cancer therapy and prompted us to

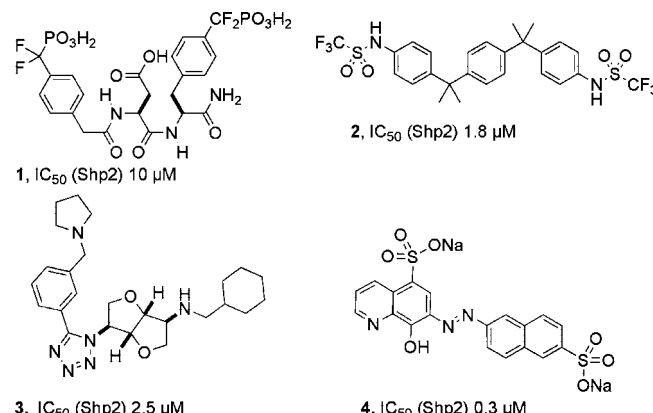


Figure 1. Known nonselective inhibitors of Shp2.

develop Shp2 inhibitors. Furthermore, the development of small molecule Shp2 inhibitors would allow us to investigate the role of Shp2 in normal and malignant processes.

The structure of the Shp2 phosphatase has been determined by X-ray crystallography at 2.0 \AA resolution.¹⁵ Shp2 contains two Src homology-2 (SH2) domains (N-SH2, C-SH2) at its N-terminal region.⁴ In the absence of a tyrosine-phosphorylated binding partner, the N-SH2 domain blocks the catalytic domain until the upstream signaling effectors bind to Shp2.¹⁵ Consequently, Shp2 is basally inactive because of autoinhibition, and inhibition of Shp2 by a small molecule is not predicted to affect resting cells, making it an attractive target for drug design.

Several compounds have been reported to nonselectively inhibit Shp2 (Figure 1). These include the potent PTP1B inhibitor **1**,¹⁶ the bis(trifluoromethylsulfonamide) **2**, which also inhibits PTP1B¹⁷ and the tetrazole **3** (NAT6-297775)¹⁸ discovered from a screen of a natural product-like library. Recently, we found that **4** (NSC-87877),²⁶ identified as a hit from the NCI Diversity set, is a potent Shp2 and Shp1 inhibitor.¹⁹ The development of a Shp2-specific inhibitor that does not cross-inhibit Shp1 is an important goal of the present study. Shp1 is mostly expressed in hematopoietic and epithelial cells and functions as a negative regulator of signaling pathways in lymphocytes.^{20,21} The crystal structure of ligand-free Shp1 shows a similar arrangement of tandem SH2 domains that adopt a conformation blocking the PTP catalytic site.²² Shp1 and Shp2 share 60% overall sequence

* To whom correspondence should be addressed. For H.R.L.: phone, 813-745-6076; fax, 813-745-6748; e-mail, Harshani.Lawrence@moffitt.org. For N.J.L.: phone, 813-745-6037; fax, 813-745-6748; e-mail, Nicholas.Lawrence@moffitt.org.

§ Drug Discovery Program, Moffitt Cancer Center.

† These authors contributed equally.

II High Throughput Screening and Chemistry Core Facility, Moffitt Cancer Center.

† Molecular Oncology Program, Moffitt Cancer Center.

V Present address: HTS Core and Division of Molecular Medicine, Beckman Research Institute, City of Hope National Medical Center, 1500E Duarte Road, Duarte, CA 91010.

‡ Department of Oncologic Sciences, University of South Florida.

V Department of Chemistry, University of South Florida.

O Department of Molecular Medicine, University of South Florida.

^a Abbreviations: Bcr-Abl, breakpoint cluster region Abelson; CagA, cytotoxin-associated gene A; c-MET, hepatocyte growth factor receptor; DiFMU, 6,8-difluoro-4-methylumbelliferyl phosphate; DIPEA, diisopropylethylamine; ErbB, avian erythroblastosis oncogene B; ERK, externally regulated kinase; GLIDE, grid-based ligand docking with energetics; NBS, N-bromosuccinimide; PTP, protein tyrosine phosphatase; SH2, Src homology-2; VEGFR, vascular endothelial growth factor receptor.

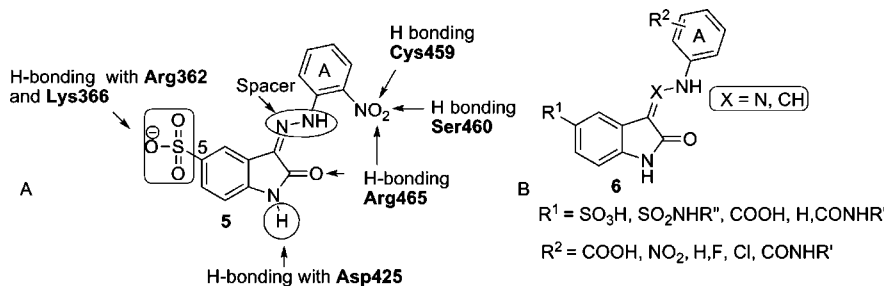


Figure 2. (A) Model of **5** representing possible important structural features for activity. (B) Structure **6** representing the oxindole pharmacophore for new inhibitor design.

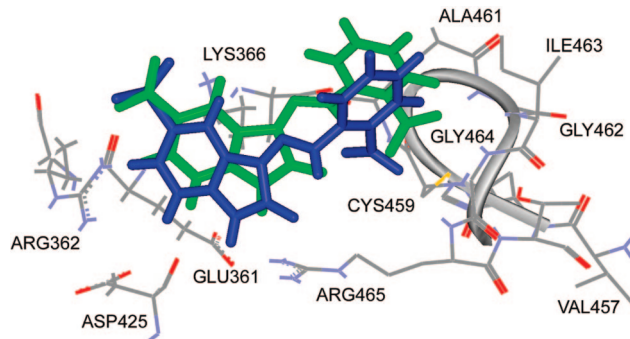


Figure 3. Overlay of **5** (blue) and **14a** (green) docked in the Shp2 PTP active site.

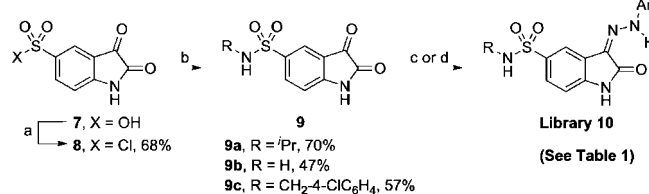
identity and approximately 75% similarity in their PTP domains.^{15,22} The Shp1 and Shp2 PTP domains are known to have different substrate specificity,^{23,24} indicating that the domains are not identical. Furthermore, the surface electrostatic potential of the catalytic cleft is much more positive in human Shp2 than in human Shp1.²⁵ Although amino acid residues presented at the base of Shp1 and Shp2 PTP catalytic clefts are identical, all four sides of the catalytic cleft contain one or more residues that are different between Shp1 and Shp2. These differences suggest that the development of a Shp2-specific PTP inhibitor, while challenging, is a realistic endeavor.

Inhibitor Design and Synthesis

We now report the development of another class of Shp2 inhibitors based on a hit from our initial screen of the NCI Diversity set. The oxindole **5** (NSC-117199)²⁶ was found to be a hit with only moderate potency ($IC_{50} = 47 \mu\text{M}$). Nevertheless, **5** was considered a reasonable hit, since it can be easily modified for library synthesis. Compounds with an oxindole core have been studied by other groups as potential therapeutic agents.^{27,28} On the basis of **5**, we have developed PTP inhibitors that display selectivity for Shp2 over Shp1 inhibition. Our primary aim, in preparing the first generation library based on the oxindole **5**, was to improve the Shp2 activity and Shp2/Shp1 selectivity. Inspection of **5** docked to Shp2 furnished a number of guidelines for analogue design. The model was obtained by docking ligands to the Shp2 PTP domain (from PDB 2SHP¹⁵) using GLIDE²⁹ and methods we have described previously.¹⁹ The model reveals the hydrazone aromatic ring system is pointing into the active site PTP signature motif³⁰ (VHCSAGIGRTG) with the polar nitro group mimicking the substrate phosphate group (Figures 2 and 3). The sulfonic acid group of the **5** is hydrogen-bonded with the basic residues Arg362 and Lys366 (Figure 2A).

The *o*-nitro group exhibited hydrogen bonding interactions with backbone atoms of the PTP loop residues Ser460, Cys459, and Arg465. The oxindole **5** appeared to fit well in the catalytic

Scheme 1^a

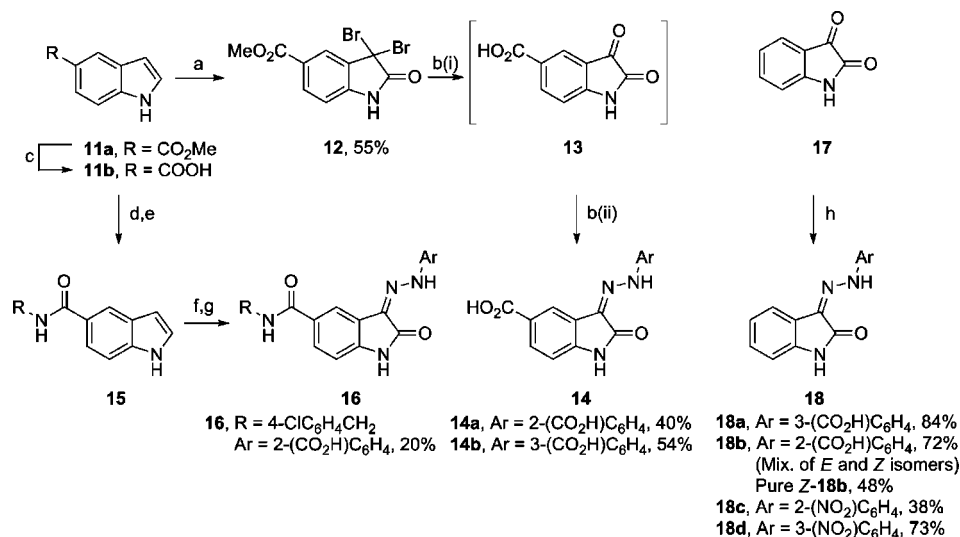


^a Reagents and conditions: (a) POCl_3 , tetramethylenesulfone, Ar, 60 °C, 3 h; (b) THF, DIPEA, RNH_2 , Ar, room temp, overnight; (c) EtOH, ArNHNNH_2 , HCl (aqueous 1 M, 2 drops) 80 °C, 4 h; (d) EtOH, ArNHNNH_2 , HCl (aqueous 1 M, 2 drops), microwave, 120 °C, 15 min.

site, suggesting that the hydrazone unit should not be replaced by longer spacer groups (Figures 2 and 3). The model also suggested the sulfonic acid could be replaced with small polar groups, e.g., sulfonamide and carboxylamide. Thus, our library was therefore biased to include small polar replacements of the nitro and sulfonic acid groups to interact with the two polar binding sites (Figure 2B). Other larger replacements (e.g., benzyl sulfonamides and benzylamides at the 5-position) were included to test to the model and to see whether only a single polar group was required. These modifications were mostly at the 2 and 3 positions of the A-ring and the C5 of the indole ring, respectively. Inclusion of sulfonamide or carboxylamide groups at the 5-position, accessible from readily available precursors, adds a useful point of diversity into the oxindole pharmacophore. The hydrogen bonding interactions of the oxindole N–H group with Asp425 was thought to be optimal, and variation of N–H was limited to N-Me. The hydrazone linker was varied by inclusion of enamine analogues (X = CH).

Several libraries of hydrazones (**10**, **14**, and **16**) were prepared by combining a 5-substituted isatin with commercially available hydrazines; the sulfonyl and carboxyl groups were elaborated with a further set of amines to provide sulfonamides and amides. The novel oxindole hydrazone sulfonamide library **10** was developed using commercially available building blocks as shown in Scheme 1. The oxindolesulfonyl chloride **8** was obtained from commercially available isatin-5-sulfonic acid according to a literature reported procedure.³¹ Isatin-5-sulfonyl chloride was coupled to a series of requisite amines to obtain the sulfonamide library **9**. We were able to isolate and analyze (NMR, mass) some members of the isatin library **9**. Attempts to purify and isolate other members of the library **9** were not successful. However, use of the crude isatinsulfonamides **9** was successful. The hydrazone library **10** was obtained by microwave assisted coupling of the crude library **9** with an appropriate set of hydrazines in moderate yields.

The carboxylic acid library **14** was prepared from methyl indole-5-carboxylate **11a** (Scheme 2). Treatment of **11a** with NBS provided the dibromoindole intermediate³² **12** in moderate yield. This was then converted into the desired library **14**

Scheme 2^a

^a Reagents and conditions: (a) NBS, isopropanol/H₂O (95:5), 0 °C, 45 min; (b) (i) HCl (aqueous 4 M, 1–3 mL), microwave, 150 °C, 5 min; (ii) HCl (aqueous 4 M, 1–3 mL), ArNHNNH₂, microwave, 150 °C, 5 min; (c) NaOH, EtOH/H₂O (1:1), 96%; (d) pentafluorophenyl trifluoroacetate, pyridine, DMF, inert conditions, room temp, 70%; (e) RNH₂, pyridine, acetonitrile, room temp; (f) NBS, isopropanol/H₂O (95:5), 0 °C, 30 min; (g) dry MeOH, ArNHNNH₂, microwave, 150 °C, 5 min (yield from 20–60%); (h) HCl (aqueous 1 M, 2 drops) EtOH, microwave, ArNHNNH₂, 120 °C, 15 min (for Z-18b irradiation time was only 2 min).

in good yields by microwave assisted coupling with the requisite hydrazines. This one-pot process occurs by hydrolysis of **12** to give the intermediate isatin **13**. Carboxylamides **15** were prepared from the pentafluorophenyl ester³³ of indole-5-carboxylic acid **11b** (Scheme 2). These amides were then reacted with NBS to form the dibromoindole³² intermediates, which were subsequently reacted with the requisite hydrazines to obtain the final library **16** as shown in Scheme 2. The syntheses of the most potent compounds are highlighted in Schemes 1 and 2. The 5-unsubstituted oxindoles **18** were synthesized in high yield by microwave assisted coupling of isatin and the required hydrazines as shown in Scheme 2. The libraries **10**, **14**, and **16** were analyzed by NMR (¹H and ¹³C) and low and high resolution mass spectroscopy. The ¹H NMR spectra of these compounds indicated formation a single stereoisomer with >95% purity. We did not observe hydrolysis of the hydrazones in routine handling and analysis of the samples. The compounds are chemically and configurationally stable in DMSO for extended periods of time at room temperature as determined by NMR (e.g., **10c** and **10h**). Isatin hydrazones have been reported to exist in the Z configuration in solution, presumably because of the intramolecular hydrogen bonding between NH of the hydrazone linkage and the carbonyl group of the indolinone.³³ The analysis of the ¹³C NMR spectra of the final compounds of the library **10** (**10a–e**, **10h**, **10i**, **10m**, **10o**, **10q**) revealed oxindole carbonyl chemical shifts around 163 ppm, indicative of the Z-hydrazone stereochemical configuration. Similarly, ¹³C NMR analysis of the library **14** also revealed carbonyl shifts around 163 ppm indicating that the members are also configured as Z. However, the reaction of isatin **17** with 2-hydrazinobenzoic acid afforded a mixture of isomers. The ¹H NMR of the compound **18b** indicated formation of a mixture of stereoisomers at approximately 1:3 ratio. Upon modifying the reaction conditions (microwave heating, 120 °C, 2 min), we see the exclusive formation (by ¹H and ¹³C NMR) of the E-configured hydrazone that was previously the minor isomer (**18c**) in 48% yield. The assignment of stereochemistry was based on observation of an NOE between the hydrazone NH and H-4 of the isatin (see Supporting Information). For comparison, no such NOE was observed for isatin **5**. So far,

we have not been able to produce the major isomer of the **18b** as a single compound. The enamine analogues **6** (X = CH) were prepared using the methods described by Kuyper and co-workers.³³ None of the enamine compounds were active (synthetic details will be presented elsewhere).

Results and Discussion

The libraries were evaluated for Shp2 PTP inhibition by in vitro PTP assay using DiFMUP as the substrate.³⁴ The compounds that displayed low micromolar inhibitory activity against Shp2 are shown in Table 1. These compounds were further screened against Shp1 and PTP1B to determine their selectivity. It was found that the carboxylic acid, sulfonamides, and carboxylamides at the 5-position of the oxindole moiety and nitro or carboxylic acid functional groups at the ortho, meta, or para position of the phenylhydrazone moiety gave rise to the best Shp2 PTP inhibitory activity. Compounds **10a–r** from the sulfonamide library with either carboxylic acid or nitro (ortho, meta, or para) groups on the aromatic hydrazone moiety showed good Shp2 inhibitory activities; IC₅₀ = 1–10 μM with >5 fold Shp2 over Shp1 selectivity. Compounds from the sulfonamide library **10** displayed better solubility under the assay conditions. The bis-carboxylic acid derivatives **14a** and **14b** displayed IC₅₀ of 0.8 and 15 μM inhibitory activity, respectively, with 20- and 5-fold Shp2 selectivity. The compounds that lack the 5-position carboxylic acid, carboxylamides or sulfonamide groups (**18a–e**, Scheme 2) showed poor activity (IC₅₀ > 60 μM, not shown in Table 1), indicating that the 5-substitution with polar groups (carboxylic acid, sulfonamide, or carboxylamide) is important for activity and suggesting that the interactions in this region with Lys366 and Arg362 (Figure 3) are pivotal. Members of both libraries **10** and **14** that possessed hydrogen, halogens (chloro or fluoro), primary amide or alkyl groups on the aromatic hydrazone moiety showed poor Shp2 inhibitory activity (not reported here), further demonstrating the importance of a carboxylate moiety (phosphotyrosine mimic) at this position and its critical role in interacting with Cys459 and Arg465. The carboxyl group when positioned at the 3 and 4 positions for the sulfonamide library generally leads to better activity. It is likely that a number of binding modes are possible,

Table 1. Shp2 Active Compounds from the Isatin Library

compd	R ¹	R ²	IC ₅₀ (μM) ^a		
			Shp2	Shp1	PTP1B
5	SO ₃ H	2-NO ₂	46.8 ± 10.2	68 ± 17.1	96.7 ± 29.9
14a	CO ₂ H	2-CO ₂ H	0.8 ± 0.2	15.4 ± 2.1	1.5 ± 0.6
14b	CO ₂ H	3-CO ₂ H	15.8 ± 6.6	72.5 ± 19.3	38.2 ± 13.9
16	CONHCH ₂ (4-ClC ₆ H ₄)	3-CO ₂ H	22.3 ± 5.2	19.4 ± 1.8	>300
10a	SO ₂ NH'Pr	3-CO ₂ H	4.5 ± 1.7	15.7 ± 1.7	37.1 ± 4.9
10b	SO ₂ NH'Pr	4-CO ₂ H	4.5 ± 1.0	27.7 ± 9.0	9.3 ± 1.6
10c	SO ₂ NH ₂	2-NO ₂	11.9 ± 1.5	103.7 ± 17.4	156.6 ± 14.1
10d	SO ₂ NHCH ₂ (4-ClC ₆ H ₄)	2-NO ₂	4.4 ± 2.4	40.9 ± 15.3	9.8 ± 2.6
10e	SO ₂ NHCH ₂ (4-MeC ₆ H ₄)	3-CO ₂ H	5.0 ± 1.9	32.6 ± 8.5	11.3 ± 4.1
10f	SO ₂ NHCH ₂ C ₆ H ₅	4-CO ₂ H	1.3 ± 0.9	7.1 ± 1.1	2.5 ± 1.5
10g	SO ₂ NHCH ₂ (3-ClC ₆ H ₄)	3-CO ₂ H	3.8 ± 0.2	42.5 ± 7.2	15.4 ± 6.2
10h	SO ₂ NHCH ₂ (4-ClC ₆ H ₄)	3-CO ₂ H	1.4 ± 0.6	18.0 ± 7.2	18.8 ± 5.1
10i	SO ₂ NHCH ₂ (4-ClC ₆ H ₄)	4-CO ₂ H	5.9 ± 1.4	18.1 ± 3.7	7.5 ± 1.1
10j	SO ₂ NHCH ₂ (2-ClC ₆ H ₄)	4-CO ₂ H	7.4 ± 2.4	60.8 ± 26.1	11.7 ± 2.4
10k	SO ₂ NHCH ₂ (2-ClC ₆ H ₄)	3-CO ₂ H	5.5 ± 0.4	15.9 ± 1.7	19.4 ± 10.2
10l	SO ₂ NHCH ₂ (3-CF ₃ -4-Cl-C ₆ H ₄)	2-CO ₂ H	22.9 ± 7.0	32.4 ± 17.9	25.7 ± 6.6
10m	SO ₂ NHCH ₂ (4-FC ₆ H ₄)	3-CO ₂ H	1.0 ± 0.2	18.3 ± 5.2	14.5 ± 1.5
10n	SO ₂ NHCH ₂ (4-FC ₆ H ₄)	4-CO ₂ H	6.3 ± 2.3	10.8 ± 4.1	11.4 ± 0.4
10o	SO ₂ NHCH ₂ (3-Cl-4-F-C ₆ H ₄)	3-CO ₂ H	4.8 ± 0.6	122.8 ± 74.5	54.9 ± 13.3
10p	SO ₂ NH(CH ₂) ₂ (2-Cl-4-ClC ₆ H ₃)	3-CO ₂ H	5.2 ± 1.7	73.4 ± 36.9	19.3 ± 13.8
10q	SO ₂ NHCH ₂ (3-CF ₃ -4-Cl-C ₆ H ₄)	4-CO ₂ H	8.3 ± 1.7	43.1 ± 7.2	32.8 ± 8.0
10r	SO ₂ NHCH ₂ (3-CF ₃ -4-Cl-C ₆ H ₄)	3-CO ₂ H	10.6 ± 1.5	74.2 ± 8.0	63.1 ± 24.7

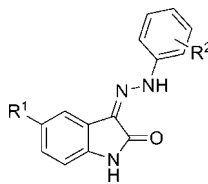
^a Values are mean values and standard deviations of at least four experiments, each performed in duplicate.

since the shallow binding pocket contains multiple positively charged residues available for interaction with a carboxyl group (e.g., Lys364, Lys366, Arg 465, Arg362, Arg 465, His426, Lys280). Varying degrees of selectivity for Shp2 versus PTP1B phosphatase inhibition were observed. For example, the potent compounds **14a** and **10f** show a 2-fold Shp2/PTP1B selectivity, whereas halosulfonamides **10g**, **10h**, and **10m** show a better 4- to 15-fold difference.

A comparison of the docking modes of **5** and **14a** is shown in Figure 3. The 5-substituents of the oxindole ring are superimposed and in the model display favorable interactions with both Lys366 and Arg362 residues and most likely contribute toward the Shp2 affinity of the ligands. The lack of activity found for all five derivatives of **18** ($IC_{50} > 60 \mu M$, Scheme 2), which lack any 5-substituents, is consistent with this observation.

The orientation of the hydrazine aromatic ring positions the carboxylic acid moiety of **14a** (Figure 3) so that it is capable of undergoing additional hydrogen bond interactions with Cys459, Gly464, and Ile463 in the catalytic site. This site binds substrate phosphoryrosine residues; therefore, it is not surprising that the carboxylate ion binds better than the nitro group. These interactions may explain the 40-fold increased potency of **14a** compared to **5** (IC_{50} values of $47 \mu M$ vs $0.8 \mu M$). The indole nitrogen atoms do not overlay well, but both show a hydrogen bonding interaction with Shp2 amino acid residues (Asp425 in the case of **5** and Glu361 with **14a**). These observations are in agreement with our design strategy to include both a polar group and phosphate mimic as a model for Shp2 inhibition.

In summary, we have identified a series of isatins capable of selectively and potently inhibiting (one compound **14a** with submicromolar activity) Shp2 over Shp1 in vitro. Furthermore the *p*-halosulfonamides **10h** and **10m** also display significant Shp2/Shp1 and Shp2/PTP1B selectivity. The SAR developed



compd	R ¹	R ²	Shp2	Shp1	PTP1B
5	SO ₃ H	2-NO ₂	46.8 ± 10.2	68 ± 17.1	96.7 ± 29.9
14a	CO ₂ H	2-CO ₂ H	0.8 ± 0.2	15.4 ± 2.1	1.5 ± 0.6
14b	CO ₂ H	3-CO ₂ H	15.8 ± 6.6	72.5 ± 19.3	38.2 ± 13.9
16	CONHCH ₂ (4-ClC ₆ H ₄)	3-CO ₂ H	22.3 ± 5.2	19.4 ± 1.8	>300
10a	SO ₂ NH'Pr	3-CO ₂ H	4.5 ± 1.7	15.7 ± 1.7	37.1 ± 4.9
10b	SO ₂ NH'Pr	4-CO ₂ H	4.5 ± 1.0	27.7 ± 9.0	9.3 ± 1.6
10c	SO ₂ NH ₂	2-NO ₂	11.9 ± 1.5	103.7 ± 17.4	156.6 ± 14.1
10d	SO ₂ NHCH ₂ (4-ClC ₆ H ₄)	2-NO ₂	4.4 ± 2.4	40.9 ± 15.3	9.8 ± 2.6
10e	SO ₂ NHCH ₂ (4-MeC ₆ H ₄)	3-CO ₂ H	5.0 ± 1.9	32.6 ± 8.5	11.3 ± 4.1
10f	SO ₂ NHCH ₂ C ₆ H ₅	4-CO ₂ H	1.3 ± 0.9	7.1 ± 1.1	2.5 ± 1.5
10g	SO ₂ NHCH ₂ (3-ClC ₆ H ₄)	3-CO ₂ H	3.8 ± 0.2	42.5 ± 7.2	15.4 ± 6.2
10h	SO ₂ NHCH ₂ (4-ClC ₆ H ₄)	3-CO ₂ H	1.4 ± 0.6	18.0 ± 7.2	18.8 ± 5.1
10i	SO ₂ NHCH ₂ (4-ClC ₆ H ₄)	4-CO ₂ H	5.9 ± 1.4	18.1 ± 3.7	7.5 ± 1.1
10j	SO ₂ NHCH ₂ (2-ClC ₆ H ₄)	4-CO ₂ H	7.4 ± 2.4	60.8 ± 26.1	11.7 ± 2.4
10k	SO ₂ NHCH ₂ (2-ClC ₆ H ₄)	3-CO ₂ H	5.5 ± 0.4	15.9 ± 1.7	19.4 ± 10.2
10l	SO ₂ NHCH ₂ (3-CF ₃ -4-Cl-C ₆ H ₄)	2-CO ₂ H	22.9 ± 7.0	32.4 ± 17.9	25.7 ± 6.6
10m	SO ₂ NHCH ₂ (4-FC ₆ H ₄)	3-CO ₂ H	1.0 ± 0.2	18.3 ± 5.2	14.5 ± 1.5
10n	SO ₂ NHCH ₂ (4-FC ₆ H ₄)	4-CO ₂ H	6.3 ± 2.3	10.8 ± 4.1	11.4 ± 0.4
10o	SO ₂ NHCH ₂ (3-Cl-4-F-C ₆ H ₄)	3-CO ₂ H	4.8 ± 0.6	122.8 ± 74.5	54.9 ± 13.3
10p	SO ₂ NH(CH ₂) ₂ (2-Cl-4-ClC ₆ H ₃)	3-CO ₂ H	5.2 ± 1.7	73.4 ± 36.9	19.3 ± 13.8
10q	SO ₂ NHCH ₂ (3-CF ₃ -4-Cl-C ₆ H ₄)	4-CO ₂ H	8.3 ± 1.7	43.1 ± 7.2	32.8 ± 8.0
10r	SO ₂ NHCH ₂ (3-CF ₃ -4-Cl-C ₆ H ₄)	3-CO ₂ H	10.6 ± 1.5	74.2 ± 8.0	63.1 ± 24.7

herein provides the basis for further optimization of the isatin library, which will be reported in due course.

Experimental Section

General. All reagents were purchased from commercial suppliers and used without further purification. Melting points were determined using a Barnstead international melting point apparatus and remain uncorrected. ¹H NMR spectra were recorded on a Varian Mercury 400 MHz spectrometer with CDCl₃ or DMSO-d₆ as the solvent. ¹³C NMR spectra are recorded at 100 MHz. All coupling constants are measured in hertz (Hz), and the chemical shifts (δ_H and δ_C) are quoted in parts per million (ppm) relative to TMS ($\delta 0$), which was used as the internal standard. High resolution mass spectroscopy was carried out on an Agilent 6210 LC/MS (ESI-TOF). Microwave reactions were performed in CEM 908005 model and Biotage initiator 8 machines. HPLC analysis was performed using a JASCO HPLC system equipped with a PU-2089 Plus quaternary gradient pump and a UV-2075 Plus UV-vis detector, using an Alltech Kromasil C-18 column (150 mm × 4.6 mm, 5 μ m). Thin layer chromatography was performed using silica gel 60 F254 plates (Fisher), with observation under UV when necessary. Anhydrous solvents (acetonitrile, dimethyl formamide, ethanol, isopropanol, methanol, and tetrahydrofuran) were used as purchased from Aldrich. HPLC grade solvents (methanol, acetonitrile, and water) were purchased from Burdick and Jackson for HPLC and mass analysis.

2,3-Dioxoindoline-5-sulfonyl Chloride 8. This compound was prepared according to a procedure reported by Lee et al.³¹ Mp = 200–202 °C (lit. mp = 188–190 °C); ³⁵¹H NMR (400 MHz, CD₃CN/CDCl₃ 1:1) δ 9.49 (br s, NH, 1H), 8.24 (dd, J = 8.4, 2.0 Hz, 1H), 8.16 (d, J = 2.0 Hz, 1H), 7.22 (d, J = 8.4 Hz, 1H).

Synthesis of Isatin Library 9. The DIPEA (2.0 mmol) and appropriate amine (1.3 mmol) were added to a solution of **8** (1.0 mmol) in anhydrous THF (8 mL) at 0 °C under inert atmosphere. The reaction mixture was warmed to room temperature and stirred overnight (some reactions required 3 days for completion). The crude reaction mixture was poured into water (10 mL) and extracted

with EtOAc (3×15 mL). The organic phase was dried (MgSO_4) and evaporated to obtain a beige/yellow solid. This crude product was taken to next stage without purification in the majority of the cases (see general procedure for library **10**) except compounds **9a**, **9b**, **9c**, which were purified by trituration with cold ethyl acetate.

2,3-Dioxo-2,3-dihydro-1*H*-indole-5-sulfonamide (9a). Yellow solid,³⁶ 47%. Mp = 198–200 °C, decomposed; ¹H NMR (400 MHz, DMSO-*d*₆) δ 7.02 (d, *J* = 8.2 Hz, 1H), 7.38 (s, 2H), 7.82 (d, *J* = 1.8 Hz, 1H), 7.95 (dd, *J* = 8.2, 1.8 Hz, 1H), 11.35 (s, 1H); ¹³C NMR (DMSO-*d*₆) δ 112.90, 118.50, 122.44, 135.74, 139.13, 153.34, 160.26, 184.00; HRMS (ESI +ve) *m/z* calculated for $\text{C}_8\text{H}_7\text{N}_2\text{O}_4\text{S}$ ($\text{M} + \text{H}$)⁺ 227.0127, found 227.0133.

2,3-Dioxo-2,3-dihydro-1*H*-indole-5-sulfonic Acid Isopropylamide (9b). Yellow solid, 70%. Mp = 184–186 °C; ¹H NMR (400 MHz, DMSO-*d*₆) δ 0.94 (d, *J* = 6.8 Hz, 6H), 3.11 (sept, *J* = 6.8 Hz, 1H), 7.04 (d, *J* = 8.2 Hz, 1H), 7.58 (d, *J* = 6.8 Hz, 1H), 7.77 (d, *J* = 1.8 Hz, 1H), 7.94 (dd, *J* = 8.2, 1.8 Hz, 1H), 11.38 (s, 1H); ¹³C NMR (DMSO-*d*₆) δ 23.90, 45.99, 113.15, 118.73, 123.00, 136.53, 136.65, 153.65, 160.20, 183.90; HRMS (ESI +ve) *m/z* calculated for $\text{C}_{11}\text{H}_{13}\text{N}_2\text{O}_4\text{S}$ ($\text{M} + \text{H}$)⁺ 269.0596, found 269.0594.

2,3-Dioxo-2,3-dihydro-1*H*-indole-5-sulfonic Acid 4-Chlorobenzylamide (9c). Yellow solid, 57%. Mp = 250 °C, decomposed; ¹H NMR (400 MHz, DMSO-*d*₆) δ 3.97 (d, *J* = 6.2 Hz, 2H), 7.00 (d, *J* = 8.1 Hz, 1H), 7.20 (d, *J* = 8.4 Hz, 2H), 7.29 (d, *J* = 8.4 Hz, 2H), 7.68 (d, *J* = 1.9 Hz, 1H), 7.89 (dd, *J* = 8.1, 1.9 Hz, 1H), 8.22 (t, *J* = 6.2 Hz, 1H), 11.41 (s, 1H); ¹³C NMR (DMSO-*d*₆) δ 46.08, 113.10, 118.57, 123.24, 128.85, 130.20, 132.40, 135.52, 136.76, 137.12, 153.75, 160.15, 183.72; HRMS (ESI +ve) *m/z* calculated for $\text{C}_{15}\text{H}_{12}\text{ClN}_2\text{O}_4\text{S}$ ($\text{M} + \text{H}$)⁺ 351.0206, found 351.0203.

General Procedure for Synthesis of Isatin Library 10. Method A. A mixture of the crude intermediate from library **9** (100 mg) and hydrazinobenzoic acid (1 equiv) in ethanol (1 mL) with hydrochloric acid (2 drops 1 M aqueous) was heated in the Biotage microwave reactor at 120 °C for 15 min. A yellow solid precipitated on cooling the reaction vial in an ice bath. The solid obtained was filtered and washed with methanol to give the pure product **10**. The yields for these two steps were in the range of 15–80%.

Method B. A mixture of the pure isatin **9a–c** (0.419 mmol) and the appropriate hydrazine (0.461 mmol) in ethanol (3 mL) with hydrochloric acid (2 drops 1 M aqueous) was heated in the Biotage microwave reactor at 120 °C for 15 min. A yellow solid was precipitated on cooling in an ice bath. The solid obtained was filtered and washed with methanol to provide the pure final product.

(Z)-3-(2-Nitrophenyl)hydrazone-2-oxoindoline-5-sulfonic Acid 5. Isatin-5-sulfonic acid (**7**) (400 mg, 1.72 mmol) and 2-nitrophenylhydrazine (296 mg, 1.65 mmol) were suspended in ethanol (10 mL), to which was added hydrochloric acid (aqueous 4 M, 4 drops). The mixture was heated under reflux for 12 h. The bright-orange precipitate obtained was filtered and washed with ethanol to provide the required product **5** (0.597 g, 93%). Mp = 272 °C, decomposed; ¹H NMR (400 MHz, DMSO-*d*₆) δ 14.21 (s, 1H, disappeared on D₂O shake), 11.23 (s, 1H, disappeared on D₂O shake), 8.24 (dd, *J* = 8.4, 0.8 Hz, 2H), 8.21 (dd, *J* = 8.4, 1.2 Hz, 1H), 7.84 (appd, *J* = 1.6 Hz, 1H), 7.79 (t, *J* = 7.6 Hz, 1H), 7.57 (dd, *J* = 8.0, 1.6 Hz, 1H), 7.19–7.14 (m, 1H), 6.87 (d, *J* = 8.0 Hz, 1H); ¹³C NMR (DMSO-*d*₆) δ 110.61, 116.59, 118.11, 120.25, 122.31, 126.46, 128.58, 133.59, 133.86, 137.33, 140.02, 142.14, 143.31, 163.38; HPLC 100% (*t*_R = 1.38, 80% methanol in water); HRMS (ESI –ve) *m/z* calculated for $\text{C}_{14}\text{H}_{9}\text{N}_4\text{O}_6\text{S}$ ($\text{M} - \text{H}$)[–] 361.0248, found 361.0250.

3-[N'-(5-Isopropylsulfamoyl)-2-oxo-1,2-dihydroindol-3-ylidene]-hydrazino]benzoic Acid (10a). **10a** was obtained by method B. Yellow solid, 57%. Mp = 275 °C, decomposed; ¹H NMR (400 MHz, DMSO-*d*₆) δ 12.76 (s, 1H, disappeared on D₂O shake), 11.43 (s, 1H, disappeared on D₂O shake), 8.05–8.06 (m, 1H), 7.92 (d, *J* = 2.0 Hz, 1H), 7.67–7.70 (m, 3H), 7.47–7.51 (d, *J* = 7.6 Hz, 2H), 7.45 (d, *J* = 8.0 Hz, 1H), 7.05 (d, *J* = 8.4 Hz, 1H), 3.21 (sept, *J* = 6.8 Hz, 1H), 0.93 (d, *J* = 6.8 Hz, 6H); ¹³C NMR (DMSO-*d*₆) δ 23.88, 45.88, 111.18, 115.36, 117.44, 119.75, 122.20, 124.74, 127.90, 127.97, 130.43, 132.79, 135.89, 143.24, 143.30, 163.76, 167.72; HPLC 99% (*t*_R = 5.20, 75% methanol in water);

HRMS (ESI –ve) *m/z* calculated for $\text{C}_{18}\text{H}_{17}\text{N}_4\text{O}_5\text{S}$ ($\text{M} - \text{H}$)[–] 401.0925, found 401.0929.

4-[N'-(5-Isopropylsulfamoyl)-2-oxo-1,2-dihydroindol-3-ylidene]-hydrazino]benzoic Acid (10b). **10b** was obtained by method B. Yellow solid, 75%. Mp = 290 °C, decomposed; ¹H NMR (400 MHz, DMSO-*d*₆) δ 12.77 (s, 1H, disappeared on D₂O shake), 12.74 (bs, 1H, disappeared on D₂O shake), 11.47 (s, 1H, disappeared on D₂O shake), 7.95 (m, 1H), 7.94 (d, *J* = 8.0 Hz, 2H), 7.70 (d, *J* = 8.0 Hz, 1H), 7.56 (1H, d, *J* = 8.0 Hz, 2H), 7.48 (d, *J* = 7.2 Hz, 1H), 7.07 (d, *J* = 8.0 Hz, 1H), 0.93 (d, *J* = 6.0 Hz, 6H); ¹³C NMR (DMSO-*d*₆) δ 23.91, 45.90, 111.35, 114.77, 117.83, 121.95, 125.72, 128.35, 129.08, 131.78, 136.02, 143.59, 146.57, 163.70, 167.56; HPLC 99.9% (*t*_R = 1.20, 90% methanol in acetonitrile); HRMS (ESI –ve) *m/z* calculated for $\text{C}_{18}\text{H}_{17}\text{N}_4\text{O}_5\text{S}$ 401.0925 ($\text{M} - \text{H}$)[–], found 401.0932.

3-[(2-Nitrophenyl)hydrazone]-2-oxo-2,3-dihydro-1*H*-indole-5-sulfonamide (10c). **10c** was obtained by method B. Yellow solid, 58%. Mp > 300 °C; ¹H NMR (400 MHz, DMSO-*d*₆) δ 14.24 (s, 1H, disappeared on D₂O shake), 11.53 (s, 1H, disappeared on D₂O shake), 8.21–8.24 (m, 1H), 8.07 (d, *J* = 1.6 Hz, 1H), 7.81–7.85 (m, 1H), 7.77 (dd, *J* = 8.0, 2.0 Hz, 1H), 7.30 (s, 2H), 7.19–7.24 (m, 1H), 7.03 (d, *J* = 8.4 Hz, 1H); ¹³C NMR (DMSO-*d*₆) δ 111.27, 116.44, 118.04, 121.18, 122.78, 126.56, 128.56, 132.74, 133.87, 137.31, 138.72, 139.63, 144.25, 163.26; HPLC 99% (*t*_R = 2.28, 90% acetonitrile in water); HRMS (ESI –ve) *m/z* calculated for $\text{C}_{14}\text{H}_{10}\text{N}_5\text{O}_5\text{S}$ ($\text{M} - \text{H}$)[–] 360.0408, found 360.0412.

3-[(2-Nitrophenyl)hydrazone]-2-oxo-2,3-dihydro-1*H*-indole-5-sulfonic Acid 4-Chlorobenzylamide (10d). **10d** was obtained by method B. Yellow solid, 43%. Mp > 300 °C; ¹H NMR (400 MHz, DMSO-*d*₆) δ 14.23 (s, 1H), 11.56 (s, 1H), 8.23–8.28 (m, 2H), 8.13 (t, *J* = 6.4 Hz, 1H), 7.90 (d, *J* 1.6 Hz, 1H), 7.82 (t, *J* = 8.4 Hz, 1H), 7.70 (dd, *J* = 8.2, 1.8 Hz, 1H), 7.23–7.27 (m, 5H), 7.06 (d, *J* = 8.0 Hz, 1H), 3.98 (d, *J* = 6.4 Hz, 2H); ¹³C NMR (DMSO-*d*₆) δ 46.14, 111.62, 116.69, 118.94, 121.39, 122.89, 126.58, 128.78, 129.59, 130.18, 132.38, 132.58, 133.95, 135.11, 137.32, 137.34, 139.69, 144.73, 163.26; HPLC 99% (*t*_R = 2.55, 90% acetonitrile in water); HRMS (ESI +ve) *m/z* calculated for $\text{C}_{21}\text{H}_{20}\text{ClN}_5\text{O}_5\text{S}$ ($\text{M} + \text{NH}_4$)⁺ 503.0904, found 503.0909; calculated for $\text{C}_{21}\text{H}_{17}\text{ClN}_5\text{O}_5\text{S}$ ($\text{M} + \text{H}$)⁺ 486.0639, found 486.0643.

(Z)-3-(2-(5-(4-Methylbenzyl)sulfamoyl)-2-oxoindolin-3-ylidene)hydrazinylbenzoic Acid (10e). **10e** was obtained by method A. Yellow solid, 27%. Mp = 297 °C, decomposed; ¹H NMR (400 MHz, DMSO-*d*₆) δ 12.77 (s, 1H, disappeared on D₂O shake), 11.43 (s, 1H, disappeared on D₂O shake), 8.07 (s, 1H), 8.02 (t, *J* = 6.4 Hz, NH, 1H, disappeared on D₂O shake), 7.84 (s, 1H), 7.72–7.62 (m, 3H), 7.49 (t, *J* = 8.0 Hz, 1H), 7.09 (d, *J* = 8.4 Hz, 2H), 7.05–7.02 (m, 3H), 5.75 (s, 1H, disappeared on D₂O shake), 3.90 (d, *J* = 6.0 Hz, 2H, CH₂, singlet on D₂O shake), 2.19 (s, CH₃, 3H); HPLC 92% (*t*_R = 1.57, 90% methanol in acetonitrile); HRMS (ESI –ve) *m/z* calculated for $\text{C}_{23}\text{H}_{19}\text{N}_4\text{O}_5\text{S}$ ($\text{M} - \text{H}$)[–] 463.1082, found 463.1087.

(Z)-4-(2-(5-(N-Benzylsulfamoyl)-2-oxoindolin-3-ylidene)hydrazinyl)benzoic Acid (10f). **10f** was obtained by method A. Yellow solid, 79%. Mp > 300 °C; ¹H NMR (400 MHz, DMSO-*d*₆) δ 12.78 (s, 1H, disappeared on D₂O shake), 11.48 (s, 1H, disappeared on D₂O shake), 8.06 (t, *J* = 8.0 Hz, NH, 1H, disappeared on D₂O shake), 7.95 (d, *J* = 8.0 Hz, 2H), 7.93 (s, 1H), 7.70 (dd, *J* = 8.0, 2.0 Hz, 1H), 7.57 (d, *J* = 8.0 Hz, 2H), 7.29–7.19 (m, 5H), 7.06 (d, *J* = 8.0 Hz, 1H), 5.70 (s, 1H, disappeared on D₂O shake), 3.96 (d, *J* = 8.0 Hz, 2H, CH₂, singlet on D₂O shake); ¹³C NMR (DMSO-*d*₆) δ 46.84, 111.33, 114.78, 118.01, 121.99, 125.73, 127.77, 128.28, 128.33, 128.54, 128.88, 131.77, 134.81, 138.28, 143.71, 146.57, 163.70, 167.56; HPLC 99% (*t*_R = 1.15, 90% methanol in acetonitrile); HRMS (ESI –ve) *m/z* calculated for $\text{C}_{22}\text{H}_{17}\text{N}_4\text{O}_5\text{S}$ ($\text{M} - \text{H}$)[–] 449.0925, found 449.0940.

(Z)-3-(2-(5-(N-Chlorobenzyl)sulfamoyl)-2-oxoindolin-3-ylidene)hydrazinylbenzoic Acid (10g). **10g** was obtained by method A. Yellow solid, 40%. Mp = 295 °C, decomposed; ¹H NMR (400 MHz, DMSO-*d*₆) δ 12.77 (s, 1H, disappeared on D₂O shake), 11.44 (s, 1H, disappeared on D₂O shake), 8.17 (t, *J* = 6.4 Hz, NH, 1H, disappeared on D₂O shake), 8.06 (s, 1H), 7.85 (d, *J* =

1.6 Hz, 1H), 7.70 (d, J = 6.4 Hz, 1H), 7.63 (d, J = 8.0 Hz, 2H), 7.49 (t, J = 8.0 Hz, 1H), 7.28–7.17 (m, 4H), 7.01 (d, J = 8.4 Hz, 1H), 5.75 (s, 1H), 4.00 (d, J = 6.4 Hz, 2H, CH_2 , singlet on D_2O shake); HPLC 99% (t_{R} = 1.63, 90% methanol in acetonitrile); HRMS (ESI –ve) m/z calculated for $\text{C}_{22}\text{H}_{16}\text{ClN}_4\text{O}_5\text{S}$ ($\text{M} - \text{H}$)[–] 483.0535, found 483.0550.

(Z)-3-(2-(5-(N-(4-Chlorobenzyl)sulfamoyl)-2-oxoindolin-3-ylidene)hydrazinyl)benzoic Acid (10h). **10h** was obtained by method A. Yellow solid, 57%. Mp > 300 °C; ¹H NMR (400 MHz, $\text{DMSO-}d_6$) δ 12.77 (s, 1H disappeared on D_2O shake), 11.43 (s, 1H disappeared on D_2O shake), 8.14 (t, J = 6.4 Hz, NH, 1H disappeared on D_2O shake), 8.06 (s, 1H), 7.82 (s, 1H), 7.71 (d, J = 8.4 Hz, 1H), 7.64 (t, J = 7.2 Hz, 2H), 7.49 (t, J = 8.0 Hz, 1H), 7.25 (dd, J = 19.2, 8.4 Hz, 4H), 7.03 (d, J = 8.4 Hz, 1H), 5.75 (s, 1H disappeared on D_2O shake), 3.96 (d, J = 6.0 Hz, 2H CH_2 , singlet on D_2O shake); ¹³C NMR ($\text{DMSO-}d_6$) δ 46.12, 111.12, 115.46, 117.59, 119.77, 122.19, 124.76, 127.77, 128.14, 128.75, 130.45, 130.46, 132.65, 132.82, 134.68, 137.36, 143.36, 143.77, 163.74, 167.72; HPLC 98.9% (t_{R} = 1.18, 90% methanol in acetonitrile); HRMS (ESI –ve) m/z calculated for $\text{C}_{22}\text{H}_{16}\text{N}_4\text{O}_5\text{S}\text{Cl}$ ($\text{M} - \text{H}$)[–] 483.0535, found 483.0536.

(Z)-4-(2-(5-(N-(4-Chlorobenzyl)sulfamoyl)-2-oxoindolin-3-ylidene)hydrazinyl)benzoic Acid (10i). **10i** was obtained by method A. Yellow solid, 55%. Mp > 300 °C; ¹H NMR (400 MHz, $\text{DMSO-}d_6$) δ 12.78 (s, 1H disappeared on D_2O shake), 11.47 (s, 1H disappeared on D_2O shake), 8.12 (t, J = 6.4 Hz, NH, 1H disappeared on D_2O shake), 7.94 (d, J = 8.0 Hz, 2H), 7.84 (s, 1H), 7.66 (d, J = 8.0 Hz, 1H), 7.57 (d, J = 8.0 Hz, 2H), 7.25 (dd, J = 17.6, 8.4 Hz, 4H), 7.04 (d, J = 7.6 Hz, 1H), 5.75 (s, 1H disappeared on D_2O shake), 3.97 (d, J = 6.4 Hz, 2H, CH_2 , singlet on D_2O shake); ¹³C NMR ($\text{DMSO-}d_6$) δ 46.12, 11.29, 114.79, 117.96, 121.94, 125.73, 128.76, 128.92, 130.15, 131.79, 131.82, 132.34, 134.82, 137.34, 143.71, 146.61, 163.68, 167.57; HRMS (ESI –ve) m/z calculated for $\text{C}_{22}\text{H}_{16}\text{ClN}_4\text{O}_5\text{S}$ ($\text{M} - \text{H}$)[–] 483.0535, found 483.0540.

(Z)-4-(2-(5-(N-(2-Chlorobenzyl)sulfamoyl)-2-oxoindolin-3-ylidene)hydrazinyl)benzoic Acid (10j). **10j** was obtained by method A. Yellow solid, 28%. Mp > 300 °C; ¹H NMR (400 MHz, $\text{DMSO-}d_6$) δ 12.77 (s, 1H, disappeared on D_2O shake), 11.47 (s, 1H, disappeared on D_2O shake), 8.14 (t, J = 5.6 Hz, NH, 1H disappeared on D_2O shake), 7.94 (d, J = 8.8 Hz, 2H), 7.92 (s, 1H), 7.69 (dd, J = 8.4, 1.6 Hz, 1H), 7.56 (d, J = 8.8 Hz, 2H), 7.42 (d, J = 7.6 Hz, 1H), 7.34 (dd, J = 7.6, 1.6 Hz, 1H), 7.29–7.21 (m, 2H), 7.05 (d, J = 8.0 Hz, 1H), 4.04 (d, J = 5.6 Hz, 2H, CH_2 , singlet on D_2O shake); HRMS (ESI –ve) m/z calculated for $\text{C}_{22}\text{H}_{16}\text{ClN}_4\text{O}_5\text{S}$ ($\text{M} - \text{H}$)[–] 483.0535, found 483.0538.

(Z)-3-(2-(5-(N-(2-Chlorobenzyl)sulfamoyl)-2-oxoindolin-3-ylidene)hydrazinyl)benzoic Acid (10k). **10k** was obtained by method A. Yellow solid, 35%. Mp > 300 °C; ¹H NMR (400 MHz, $\text{DMSO-}d_6$) δ 12.77 (s, 1H, disappeared on D_2O shake), 11.44 (s, 1H, disappeared on D_2O shake), 8.16 (t, J = 5.6 Hz, NH, 1H disappeared on D_2O shake), 8.07 (s, 1H), 7.90 (d, J = 1.2 Hz, 1H), 7.69 (dt, J = 8.4, 2.0 Hz, 2H), 7.63 (d, J = 8.0 Hz, 1H), 7.49 (t, J = 8.0 Hz, 1H), 7.38 (dd, J = 7.6, 2.0 Hz, 1H), 7.33 (dd, J = 7.2, 1.2 Hz, 1H), 7.29–7.21 (m, 2H), 7.05 (d, J = 8.0 Hz, 1H), 5.75 (s, 1H, disappeared on D_2O shake), 3.96 (d, J = 5.6 Hz, 2H, CH_2 , singlet on D_2O shake); HRMS (ESI –ve) m/z calculated for $\text{C}_{22}\text{H}_{16}\text{ClN}_4\text{O}_5\text{S}$ ($\text{M} - \text{H}$)[–] 483.0535, found 483.0541.

(Z)-2-(2-(5-(N-(4-Chloro-3-(trifluoromethyl)benzyl)sulfamoyl)-2-oxoindolin-3-ylidene)hydrazinyl)benzoic Acid (10l). **10l** was obtained by method A. Yellow solid, 35%. Mp > 300 °C; ¹H NMR (400 MHz, $\text{DMSO-}d_6$) δ 14.25 (s, 1H disappeared on D_2O shake), 11.30 (s, 1H, disappeared on D_2O shake), 8.24 (t, J = 6.4 Hz, NH, 1H disappeared on D_2O shake), 8.04 (d, J = 8.4 Hz, 1H), 7.95 (dd, J = 8.0, 1.6 Hz, 1H), 7.74 (d, J = 1.6 Hz, 1H), 7.66, (t, J = 7.6 Hz, 1H), 7.60–7.52 (m, 4H), 7.12 (t, J = 7.6 Hz, 1H), 6.95 (d, J = 8.0 Hz, 1H), 4.14 (d, J = 6.4 Hz, 2H, CH_2 , singlet on D_2O shake); HRMS (ESI –ve) m/z calculated for $\text{C}_{23}\text{H}_{15}\text{ClF}_3\text{N}_4\text{O}_5\text{S}$ ($\text{M} - \text{H}$)[–] 551.0409, found 551.0414.

(Z)-3-(2-(5-(N-(4-Fluorobenzyl)sulfamoyl)-2-oxoindolin-3-ylidene)hydrazinyl)benzoic Acid (10m). **10m** was obtained by method A. Yellow solid, 40%. Mp > 300 °C; ¹H NMR (400 MHz, $\text{DMSO-}d_6$) δ 12.76 (s, 1H disappeared on D_2O shake), 11.43 (s, 1H disappeared on D_2O shake), 8.10 (t, J = 6.4 Hz, NH, 1H disappeared on D_2O shake), 8.06 (s, 1H), 7.86 (s, 1H), 7.70 (d, J = 7.6 Hz, 1H), 7.64 (t, J = 8.8 Hz, 2H), 7.49 (t, J = 7.6 Hz, 1H), 7.25 (dd, J = 8.0, 5.6 Hz, 2H), 7.08–7.02 (m, 3H), 3.94 (d, J = 6.4 Hz, 2H, CH_2 , singlet on D_2O shake); ¹³C NMR ($\text{DMSO-}d_6$) δ 46.07, 111.12, 115.42, 115.55 (d, J = 21 Hz), 117.56, 119.78, 122.20, 124.76, 127.75, 128.16, 130.29 (d, J = 8 Hz), 130.45, 132.79, 134.49 (d, J = 3 Hz), 134.64, 143.31, 143.35, 161.97 (d, J = 241 Hz), 163.72, 167.72; HPLC 99% (t_{R} = 1.45, 90% methanol in acetonitrile); HRMS (ESI –ve) m/z calculated for $\text{C}_{22}\text{H}_{16}\text{FN}_4\text{O}_5\text{S}$ ($\text{M} - \text{H}$)[–] 467.0831, found 467.0844.

(Z)-4-(2-(5-(N-(4-Fluorobenzyl)sulfamoyl)-2-oxoindolin-3-ylidene)hydrazinyl)benzoic Acid (10n). **10n** was obtained by method A. Yellow solid, 41%. Mp > 300 °C; ¹H NMR (400 MHz, $\text{DMSO-}d_6$) δ 12.77 (s, 1H disappeared on D_2O shake), 11.46 (s, 1H disappeared on D_2O shake), 8.07 (t, J = 6.4 Hz, NH, 1H disappeared on D_2O shake), 7.93 (d, J = 8.8 Hz, 2H), 7.88 (s, 1H), 7.67 (dd, J = 8.4, 1.2 Hz, 1H), 7.56 (d, J = 8.4 Hz, 2H), 7.27–7.23 (m, 2H), 7.08–7.03 (m, 3H), 3.95 (d, J = 6.4 Hz, 2H, CH_2 , singlet on D_2O shake); HPLC 96% (t_{R} = 1.43, 90% methanol in acetonitrile); HRMS (ESI –ve) m/z calculated for $\text{C}_{22}\text{H}_{16}\text{FN}_4\text{O}_5\text{S}$ ($\text{M} - \text{H}$)[–] 467.0831, found 467.0846.

(Z)-3-(2-(5-(N-(3-Chloro-4-fluorobenzyl)sulfamoyl)-2-oxoindolin-3-ylidene)hydrazinyl)benzoic Acid (10o). **10o** was obtained by method B. Yellow solid, 87%. Mp = 293–295 °C; ¹H NMR (400 MHz, $\text{DMSO-}d_6$) δ 12.76 (s, 1H disappeared on D_2O shake), 11.43 (s, 1H, disappeared on D_2O shake), 8.17 (t, J = 5.6 Hz, NH, 1H disappeared on D_2O shake), 8.01 (s, 1H), 7.79 (s, 1H), 7.70 (d, J = 6.8 Hz, 1H), 7.64–7.58 (m, 2H), 7.49 (t, J = 7.6 Hz, 1H), 7.30 (d, J = 8.0 Hz, 1H), 7.24–7.22 (m, 2H), 6.99 (d, J = 8.8 Hz, 1H), 3.99 (d, J = 5.6 Hz, 2H, CH_2 , singlet on D_2O shake); ¹³C NMR ($\text{DMSO-}d_6$) δ 45.59, 111.06, 115.44, 117.03, 117.24, 117.51, 119.61, 119.79, 122.17, 124.77, 127.68, 128.11, 128.98 (d, J = 7 Hz), 130.35 (d, J = 15 Hz), 132.79, 134.72, 136.15 (d, J = 3 Hz), 143.34 (d, J = 6 Hz), 156.88 (d, J = 244 Hz), 163.70, 167.72; HRMS (ESI –ve) m/z calculated for $\text{C}_{22}\text{H}_{15}\text{ClF}_4\text{N}_4\text{O}_5\text{S}$ ($\text{M} - \text{H}$)[–] 501.0441, found 501.0437.

(Z)-3-(2-(5-(N-(2,4-Dichlorophenethyl)sulfamoyl)-2-oxoindolin-3-ylidene)hydrazinyl)benzoic Acid (10p). **10p** was obtained by method A. Yellow solid, 14%. Mp = 290–292 °C; ¹H NMR (400 MHz, $\text{DMSO-}d_6$) δ 12.77 (s, 1H disappeared on D_2O shake), 11.43 (s, 1H disappeared on D_2O shake), 8.07 (s, 1H), 7.82 (s, 1H), 7.71 (d, J = 6.4 Hz, 2H), 7.64–7.61 (m, 2H, integrated to 1H on D_2O shake), 7.50 (t, J = 8.4 Hz, 1H), 7.44 (d, J = 1.6 Hz, 1H), 7.31–7.25 (m, 2H), 7.03 (d, J = 8.4 Hz, 1H), 5.75 (s, 1H disappeared on D_2O shake), 2.99 (q, J = 6.4 Hz, 2H, CH_2 , triplet on D_2O shake), 2.76 (t, J = 6.4 Hz, 2H, CH_2); HRMS (ESI –ve) m/z calculated for $\text{C}_{23}\text{H}_{17}\text{Cl}_2\text{N}_4\text{O}_5\text{S}$ ($\text{M} - \text{H}$)[–] 531.0302, found 531.0304.

(Z)-4-(2-(5-(N-(4-Chloro-3-(trifluoromethyl)benzyl)sulfamoyl)-2-oxoindolin-3-ylidene)hydrazinyl)benzoic Acid (10q). **10q** was obtained by method A. Yellow solid, 34%. Mp > 300 °C; ¹H NMR (400 MHz, $\text{DMSO-}d_6$) δ 12.76 (s, 1H disappeared on D_2O shake), 11.44 (s, 1H disappeared on D_2O shake), 8.25 (t, J = 6.4 Hz, NH, 1H disappeared on D_2O shake), 7.94 (d, J = 8.8 Hz, 2H), 7.70 (s, 1H), 7.58–7.52 (m, 6H), 6.95 (d, J = 8.4 Hz, 1H), 5.75 (s, 1H disappeared on D_2O shake), 4.13 (d, J = 6.4 Hz, 2H, CH_2 , singlet on D_2O shake); ¹³C NMR ($\text{DMSO-}d_6$) δ 45.72, 111.15, 114.76, 117.90, 121.79, 125.73, 126.04 (q, J = 272 Hz), 126.64, 126.94, 127.46 (d, J = 5 Hz), 128.37, 128.72, 131.76, 131.93, 134.10, 134.93, 138.27, 143.68, 146.59, 163.64, 167.58; HRMS (ESI –ve) m/z calculated for $\text{C}_{23}\text{H}_{15}\text{ClF}_3\text{N}_4\text{O}_5\text{S}$ ($\text{M} - \text{H}$)[–] 551.0409, found 551.0404.

(Z)-3-(2-(5-(N-(4-Chloro-3-(trifluoromethyl)benzyl)sulfamoyl)-2-oxoindolin-3-ylidene)hydrazinyl)benzoic Acid (10r). **10r** was obtained by method A. Yellow solid, 40%. Mp = 292–294 °C; ¹H NMR (400 MHz, $\text{DMSO-}d_6$) δ 12.75 (s, 1H disappeared on

D₂O shake), 11.41 (s, 1 H disappeared on D₂O shake), 8.28 (t, *J* = 6.4 Hz, NH, 1H disappeared on D₂O shake), 8.05 (s, 1H), 7.70–7.68 (m, 2H), 7.63 (d, *J* = 7.6 Hz, 1H), 7.57–7.47 (m, 5H), 6.95 (d, *J* = 8.0 Hz, 1H), 4.12 (d, *J* = 6.4 Hz, 2H, CH₂, singlet on D₂O shake); HRMS (ESI –ve) *m/z* calculated for C₂₃H₁₅ClF₃N₄O₅S (M – H)[–] 551.0409, found 551.0420.

3,3-Dibromo-2-oxo-2,3-dihydro-1*H*-indole-5-carboxylic Acid Methyl Ester (12). *N*-Bromosuccinimide (13.41 g, 74.91 mmol) was added portionwise to a solution of 5-methyl indole-2-carboxylate (**11a**) (4.50 g, 25.71 mmol) in isopropanol/H₂O (95:5, 350 mL) over 45 min under argon at room temperature. After the addition, the solvent was removed under reduced pressure and the solid residue was triturated with cold acetone (150 mL) to give the pure product as a yellow solid (4.90 g, 55%). Mp > 300 °C; ¹H NMR (400 MHz, DMSO-*d*₆) *δ* 11.71 (s, 1H), 8.05 (d, *J* = 1.5 Hz, 1H), 7.98 (dd, *J* = 8.2, 1.5 Hz, 1H), 7.06 (d, *J* = 8.2 Hz, 1H), 3.86 (s, 3H); ¹³C NMR (DMSO-*d*₆) *δ* 52.92, 111.96, 125.37, 126.83, 132.08, 134.15, 143.28 (2C), 165.88, 171.27.

(Z)-3-(2-(2-Carboxyphenyl)hydrazone)-2-oxoindoline-5-carboxylic Acid (14a). Methyl dibromoindole carboxylate **9** (40 mg, 0.114 mmol) was suspended in HCl (aqueous 4 M, 2.00 mL) in a microwave vial and heated at 150 °C for 5 min. The intermediate **13** was not isolated (Scheme 2). 2-Hydrazinylbenzoic acid (23 mg, 0.126 mmol) was added to the reaction mixture and heated using the Biotage microwave reactor at 150 °C for 15 min. The solid obtained upon cooling the reaction vial was filtered and washed with DCM to obtain the pure **14a** (15 mg, 40%) as an off-white solid. Mp > 300 °C; ¹H NMR (400 MHz, DMSO-*d*₆) *δ* 14.22 (s, 1H, disappeared on D₂O shake), 11.27 (s, 1H, disappeared on D₂O shake), 8.11 (appd, *J* = 1.2 Hz, 1H), 8.07 (d, *J* = 8.4 Hz, 1H), 7.93 (dd, *J* = 8.0, 1.2 Hz), 7.87 (dd, *J* = 8.0, 1.2 Hz, 1H), 7.63 (t, *J* = 8.4 Hz, 1H), 7.09 (t, *J* = 7.2 Hz, 1H), 6.99 (d, *J* = 8.4 Hz, 1H); ¹³C NMR (DMSO-*d*₆) *δ* 110.94, 114.55, 114.88, 120.71, 121.93, 122.48, 124.98, 129.82, 131.53, 131.97, 135.21, 144.74, 145.26, 163.04, 167.82, 168.91; HPLC 100% (*t*_R = 1.55, 80% methanol in water); HRMS (ESI –ve) *m/z* calculated for C₁₆H₁₀N₃O₅ (M – H)[–] 324.0625, found 324.0622.

(Z)-3-(2-(3-Carboxyphenyl)hydrazone)-2-oxoindoline-5-carboxylic Acid (14b). The procedure was same as for the compound **14a**. 3-Hydrazinylbenzoic acid (23 mg, 0.126 mmol) was used to obtain the final compound **14b** (20 mg, 54%) as an off-white solid. Mp > 300 °C; ¹H NMR (400 MHz, DMSO-*d*₆) *δ* 12.97 (broad s, 1H, disappeared on D₂O shake), 12.70 (s, 1H, disappeared on D₂O shake), 11.37 (s, 1H, disappeared on D₂O shake), 8.06 (s, 1H), 8.00 (s, 1H), 7.86 (dd, *J* = 8.0, 1.2 Hz, 1H), 7.72 (d, *J* = 8.0 Hz, 1H), 7.60 (d, *J* = 7.6 Hz, 1H), 7.49–7.45 (m, 1H), 7.00 (d, *J* = 8.4 Hz, 1H); HPLC 100% (*t*_R = 1.60, 80% methanol in water); HRMS (ESI –ve) *m/z* calculated for C₁₆H₁₀N₃O₅ (M – H)[–] 325.0625, found 324.0635.

Pentafluorophenyl 1*H*-Indole-5-carboxylate, Intermediate for 15. To a solution of 5-indolecarboxylic acid (0.5 g, 3.10 mmol) in DMF (3.00 mL) was added pentafluorophenyl trifluoroacetate (1.068 mL, 6.20 mmol) followed by pyridine (0.281 mL). The reaction mixture (a suspension was obtained at this stage) was stirred at room temperature under inert atmosphere for approximately 30 min. The reaction mixture was poured into ether (40 mL) and diluted with ethyl acetate (2 × 50 mL). The organic phase was washed with water, dried (Na₂SO₄), and concentrated to obtain an off-white solid (720 mg, 70%), TLC *R*_F = 0.71 (EtOAc/hexane, 1:1). No purification was necessary: ¹H NMR (400 MHz, DMSO-*d*₆) *δ* 11.71 (s, 1H, NH), 8.49 (s, 1H), 7.85 (dd, *J* = 8.4, 2.0 Hz, 1H), 7.59–7.55 (m, 2H), 6.67 (broad t, 1H).

N-(4-Chlorobenzyl)-1*H*-indole-5-carboxamide (15). The pentafluorophenyl ester (200 mg, 0.61 mmol) from the above experiment was suspended in dry acetonitrile under argon. Pyridine (0.075 mL, 0.85 mmol) was added followed by 4-chlorobenzylamine (121 mg, 0.85 mmol) and stirred overnight (approximately 12 h). The resulting cloudy solution was diluted with EtOAc and washed with HCl (4 M aqueous, 6 mL). The organic phase was separated, washed with water, dried (Na₂SO₄), and concentrated to give the intermediate **15** (252 mg) as an orange solid. This compound

was used in the next step without further purification. ¹H NMR (400 MHz, DMSO-*d*₆) *δ* 11.40 (s, 1H, disappeared on D₂O shake), 11.32 (s, 1H), 8.91 (t, *J* = 6.4 Hz, 1H, changed on D₂O shake), 8.15 (s, 1H), 7.64 (dd, *J* = 8.4, 1.2 Hz, 1H), 7.40–7.31 (m, 5H), 6.51 (m, 1H), 4.45 (d, *J* = 6.0 Hz, 2H, singlet on D₂O shake).

3,3-Dibromo-N-(4-chlorobenzyl)-2-oxoindoline-5-carboxamide, Intermediate for 16. The indole **15** (252 mg, 0.89 mmol) was dissolved in aqueous isopropanol/H₂O (95:5, 5 mL), and NBS (0.471 g, 2.65 mmol) was added portionwise over 30 min with stirring under argon atmosphere. The reaction was monitored by TLC (EtOAc/hexane, 1:1). TLC indicated the disappearance of the starting material. The reaction mixture was concentrated at room temperature and diluted with ether (approximately 10 mL). The succinimide precipitate was filtered and washed with ether. The ether phase was concentrated to obtain a pale-yellow solid (225 mg, 55%). Attempts to purify this intermediate were not successful. The crude compound was used in the next step.

(Z)-3-(2-(5-(4-Chlorobenzylcarbamoyl)-2-oxoindolin-3-ylidene)-hydrazinyl)benzoic Acid (16). The crude dibromoindole intermediate from the above experiment (70 mg, 0.152 mmol) was suspended in dry MeOH (2.0 mL) in a microwave vial (CEM, 10.0 mL), and 3-hydrazinylbenzoic acid (31 mg, 0.166 mmol) was added and irradiated for 5 min at 150 °C in the CEM microwave reactor. The reaction vial was left in an ice bath until a precipitate formed. The compound **16** (15 mg, 22%) was isolated as a pale-yellow solid. Mp > 300 °C; ¹H NMR (400 MHz, DMSO-*d*₆) *δ* 13.10 (broad s, 1H, disappeared on D₂O shake), 12.79 (s, 1H, disappeared on D₂O shake), 11.31 (s, 1H, disappeared on D₂O shake), 9.13 (broad t, 1H), 8.12 (s, 1H), 8.04 (s, 1H), 7.84 (d, *J* = 8.4 Hz, 1H), 7.67 (d, *J* = 6.8 Hz, 1H), 7.61 (d, *J* = 7.6 Hz, 1H), 7.48 (t, *J* = 6.8 Hz, 1H), 7.37–7.33 (m, 4H), 6.99 (d, *J* = 8.0 Hz, 1H), 4.45 (d, *J* = 5.2 Hz, 2H); HPLC 95% (*t*_R = 1.70, 80% methanol in water); LRMS (ESI +ve) *m/z* 449 [100, (M + H⁺)]; HRMS (ESI –ve) *m/z* calculated for C₂₃H₁₇ClN₄O₄ (M – H)[–] 447.0860, found 447.0861.

(Z)-3-(2-(2-Oxoindolin-3-ylidene)hydrazinyl)benzoic Acid (18a). A mixture of isatin (0.111 g, 0.775 mmol) and 3-carboxyphenylhydrazine (0.085 g, 0.160 mmol) and HCl (aqueous 1 M, 2 drops) in ethanol (3 mL) was heated in the Biotage microwave at 120 °C for 15 min. After the mixture was cooled to room temperature, pure product **18a** was collected as a yellow precipitate by filtration and dried in vacuo (0.184 g, 0.65 mmol, 84%). Yellow solid, 84%. Mp > 300 °C; ¹H NMR (400 MHz, DMSO-*d*₆) *δ* 13.05 (broad s, 1H), 12.77 (s, 1H), 11.04 (s, 1H), 9.91 (d, *J* = 8.0 Hz, 1H), 7.96 (s, 1H), 7.54–7.64 (m, 3H), 7.44 (t, *J* = 8.0 Hz, 1H), 7.24 (t, *J* = 7.2 Hz, 1H), 7.04 (t, *J* = 8.0 Hz, 1H); ¹³C NMR (100 MHz, DMSO-*d*₆) *δ* 111.23, 115.06, 119.16, 119.54, 121.66, 122.62, 124.12, 129.24, 129.52, 130.39, 132.74, 140.77, 143.57, 163.75, 167.75; HRMS (ESI –ve) *m/z* calculated for C₁₅H₁₀N₃O₃ (M – H)[–] 280.0727, found 280.0736.

(E) and (Z)-2-(2-Oxoindolin-3-ylidene)hydrazinyl)benzoic Acid (18b). A mixture of isatin (**17**) (0.074 g, 0.517 mmol), 2-carboxyphenylhydrazine (0.107 g, 0.568 mmol), and HCl (aqueous 1 M, 2 drops) in ethanol (3 mL) was heated in the Biotage microwave reactor at 120 °C for 15 min. After the mixture was cooled to room temperature, hydrazone **18b** (0.057 g, 0.20 mmol, 72%) was collected as a mixture of isomers (Z/E 3:1) as a yellow precipitate by filtration and dried in vacuo. ¹H NMR (400 MHz, DMSO-*d*₆) *δ* 14.19 (s, 1H), 10.92 (s, 1H), 8.01 (d, *J* = 8.0 Hz, 1H), 7.92 (d, *J* = 7.6 Hz, 1H), 7.58–7.69 (m, 2H, overlap with the minor isomer), 7.25 (t, *J* = 7.6 Hz, 1H), 7.21–7.11 (m, 2H, overlap with the minor isomer), 6.90 (d, *J* = 6.8 Hz, 1H); minor isomer (*E*) (25%) *δ* 12.39 (s, 1H), 10.72 (s, 1H), 8.04 (d, *J* = 8.0 Hz, 1H), 7.97 (dd, *J* = 8.0 Hz, 1H), 7.85 (d, *J* = 8.4 Hz, 1H), 7.58–7.69 (m, 1H, overlap with the major isomer), 7.37 (t, *J* = 7.2 Hz, 1H), 7.21–7.11 (m, 2H, overlap with the major isomer), 6.94 (d, *J* = 7.2 Hz, 1H); HRMS (ESI –ve) *m/z* calculated for C₁₅H₁₀N₃O₃ (M – H)[–] 280.0727, found 280.0732.

(E)-2-(2-(2-Oxoindolin-3-ylidene)hydrazinyl)benzoic Acid (18b).

A mixture of isatin (17) (0.060 g, 0.419 mmol), 2-carboxylphenylhydrazine (0.085 g, 0.461 mmol), and HCl (aqueous 1 M, 2 drops) in ethanol (3 mL) was heated in the Biotage microwave reactor at 120 °C for 2 min. After the mixture was cooled to room temperature, pure product **18b** was collected as a yellow precipitate by filtration and dried in vacuo (0.057 g, 0.20 mmol, 48%). Mp > 300 °C; ¹H NMR (400 MHz, DMSO-*d*₆) δ 12.41 (s, 1H), 10.71 (s, 1H), 8.04 (d, *J* = 6.8 Hz, 1H), 7.97 (dd, *J* = 1.2, 8.0 Hz, 1H), 7.85 (d, *J* = 8.4 Hz, 1H), 7.64–7.68 (m, 1H), 7.37 (t, *J* = 7.6 Hz, 1H), 7.06 (m, 2H), 6.94 (d, *J* = 7.6 Hz, 1H); ¹³C NMR (DMSO-*d*₆) δ 111.33, 133.33, 114.38, 116.43, 121.97, 122.21, 122.82, 131.72, 131.97, 132.72, 135.56, 142.87, 146.20, 165.60, 170.63; HRMS (ESI –ve) *m/z* calculated for C₁₅H₁₀N₃O₃ (M – H)[–] 280.0727, found 280.0736.

(Z)-3-(2-(2-Nitrophenyl)hydrazine)indolin-2-one (18c). A mixture of isatin (17) (200 mg, 1.35 mmol), 2-nitrophenylhydrazine (226 mg 1.48 mmol, and HCl (aqueous 4 M, 4 drops) in ethanol (26.0 mL) was heated under reflux for 2 h. The reaction mixture was cooled to room temperature and the yellow solid was filtered and washed with ethanol to obtain the pure product **18c** as an orange solid (145 mg, 38%). Mp = 279 °C, decomposed; ¹H NMR (400 MHz, DMSO-*d*₆) δ 11.56 (s, 1H, disappeared on D₂O shake), 10.84 (s, 1H, disappeared on D₂O shake), 8.22 (d, *J* = 7.2 Hz, 1H), 8.01 (d, *J* = 8.4 Hz, 1H), 7.87–7.80 (m, 2H), 7.44–7.40 (m, 1H), 7.18 (q, *J* = 14.4, 7.2 Hz, 2H), 6.96 (d, *J* = 7.6 Hz, 1H); ¹³C NMR (DMSO-*d*₆) δ 111.76, 116.27, 116.66, 122.44, 122.68, 123.69, 126.60, 132.92, 134.18, 135.96, 137.43, 140.57, 143.85, 165.17; HRMS (ESI +ve) *m/z* calculated for C₁₄H₁₁N₄O₃ (M + H)⁺ 283.0826, found 283.0834.

(Z)-3-(2-(3-Nitrophenyl)hydrazine)indolin-2-one (18d). A mixture of isatin (17) (200 mg, 1.35 mmol), 2-nitrophenylhydrazine (226 mg, 1.48 mmol), and HCl (aqueous 4 M, 4 drops) in ethanol (26.0 mL) was heated under reflux for 2 h. The reaction mixture was cooled to room temperature and the yellow solid was filtered and washed with ethanol to obtain the pure product **18d** (279 mg, 73%) as a yellow solid. Mp = 267–269 °C; ¹H NMR (400 MHz, DMSO-*d*₆) δ 12.75 (s, 1H), 11.07 (s, 1H), 8.25 (t, *J* = 4.0 Hz, 1H), 7.85 (ddd, *J* = 8.0, 2.8, 0.8 Hz, 1H), 7.81 (ddd, *J* = 8.0, 2.0, 0.8 Hz, 1H), 7.62–7.57 (m, 2H), 7.26 (td, *J* = 7.6, 1.2 Hz, 1H), 7.04 (td, *J* = 7.2, 1.2 Hz, 1H), 6.90 (d, *J* = 7.6 Hz, 1H); ¹³C NMR (DMSO-*d*₆) δ 108.91, 111.30, 117.34, 119.95, 121.14, 122.71, 130.07, 130.53, 131.53, 141.24, 144.24, 144.80, 149.46, 163.49; HRMS (ESI +ve) *m/z* calculated for C₁₄H₁₁N₄O₃ (M + H)⁺ 283.0826, found 283.0835.

Phosphatase Activity. PTP activity was measured using the fluorogenic 6, 8-difluoro-4-methylumbelliferyl phosphate (DiFMUP, from Molecular Probes) as the substrate. Each reaction contained 25 mM MOPS (pH 7.0), 50 mM NaCl, 0.05% Tween-20, 1 mM DTT, 20 μM DiFMUP, 10 nM Microcystin LR, 20 nM PTP (Shp2, Shp1 or PTP1B),¹⁹ and 5 μL of test compound or dimethyl sulfoxide (DMSO, solvent) in a total reaction volume of 100 μL in a black 96-well plate. Reaction was initiated by addition of DiFMUP, and the incubation time was 30 min at room temperature. DiFMUP fluorescence signal was measured at an excitation of 355 nm and an emission of 460 nm with a Wallac Victor² 1420 plate reader. IC₅₀ was defined as the concentration of an inhibitor that caused a 50% decrease in the PTP activity. For IC₅₀ determination, eight concentrations of compounds at 1/3 dilution (~0.5 log) were tested. Each experiment was performed in duplicate, and IC₅₀ data were derived from at least four independent experiments. The curve-fitting program Prism 4 (GraphPad Software) was used to calculate the IC₅₀ value.

Acknowledgment. This work was supported by NIH Grants P01CA118210, R01CA077467 and P30CA076292-10 (Cancer Center Support Grant).

Supporting Information Available: Characterization data, mass and NMR spectra, and HPLC traces of compounds **5**, **10a–r**, **14a,b**, **17**, and **18a–e**, NOE and COSY data for **5** and **18c**, and a

description of the molecular modeling studies. This material is available free of charge via the Internet at <http://pubs.acs.org>.

Note Added in Proof. Birchmeier and co-workers have recently described the virtual screening based discovery of several phenylhydrazonepyrazolone derivatives as Shp2 inhibitors. See Hellmuth, K.; Grosskopf, S.; Lum, C. T.; Wuertele, M.; Roeder, N.; von Kries, J. P.; Rosario, M.; Rademann, J.; Birchmeier, W. Specific inhibitors of the protein tyrosine phosphatase Shp2 identified by high-throughput docking. *Proc. Natl. Acad. Sci. U. S. A.* **2008**, *105*, 7275–7280.

References

- Bridges, A. J. Chemical inhibitors of protein kinases. *Chem. Rev.* **2001**, *101*, 2541–2571.
- (a) Bialy, L.; Waldmann, H. Inhibitors of protein tyrosine phosphatases: next-generation drugs. *Angew. Chem. Int. Ed.* **2005**, *44*, 3814–3839. (b) Jiang, Z.-X.; Zhang, Z.-Y. Targeting PTPs with small molecule inhibitors in cancer treatment. *Cancer Metastasis Rev.* **2008**, *27*, 263–272. (c) Tautz, L.; Pellecchia, M.; Mustelin, T. Targeting the PTpome in human disease. *Expert Opin. Ther. Targets* **2006**, *10*, 157–177. (d) Dewang, P. M.; Hsu, N. M.; Peng, S. Z.; Li, W. R. Protein tyrosine phosphatases and their inhibitors. *Curr. Med. Chem.* **2005**, *12*, 1–22. (e) Tautz, L.; Mustelin, T. Strategies for developing protein tyrosine phosphatase inhibitors. *Methods* **2007**, *42*, 250–260.
- (3) Alonso, A.; Sasin, J.; Bottini, N.; Friedberg, I.; Friedberg, I.; Osterman, A.; Godzik, A.; Hunter, T.; Dixon, J.; Mustelin, T. Protein tyrosine phosphatases in the human genome. *Cell* **2004**, *117*, 699–711.
- (4) (a) Chan, G.; Kalaitzidis, D.; Neel, B. G. The tyrosine phosphatase Shp2 (PTPn11) in cancer. *Cancer Metastasis Rev.* **2008**, *27*, 179–192. (b) Mohi, M. G.; Neel, B. G. The role of Shp2 (PTPn11) in cancer. *Curr. Opin. Genet. Dev.* **2007**, *17*, 23–30. (c) Mannell, H.; Kroetz, F. The role of SHP-2 in cell signaling and human disease. *Curr. Enzyme Inhib.* **2007**, *3*, 264–272. (d) Neel, B. G.; Gu, H.; Pao, L. The “Shp”ing news: SH2 domain-containing tyrosine phosphatases in cell signaling. *Trends Biochem. Sci.* **2003**, *28*, 284–293.
- (5) (a) Dance, M.; Montagner, A.; Salles, J.-P.; Yart, A.; Raynal, P. The molecular functions of Shp2 in the Ras/mitogen-activated protein kinase (ERK1/2) pathway. *Cell. Signalling* **2008**, *20*, 453–459. (b) Chong, Z. Z.; Maiese, K. The Src homology 2 domain tyrosine phosphatases SHP-1 and SHP-2: diversified control of cell growth, inflammation, and injury. *Histol. Histopathol.* **2007**, *22*, 1251–1267. (c) Xu, R. Shp2, a novel oncogenic tyrosine phosphatase and potential therapeutic target for human leukemia. *Cell Res.* **2007**, *17*, 295–297. (d) Feng, G. S. Shp-2 tyrosine phosphatase: signaling one cell or many. *Exp. Cell Res.* **1999**, *253*, 47–54.
- (6) Nishida, K.; Hirano, T. The role of Gab family scaffolding adapter proteins in the signal transduction of cytokine and growth factor receptors. *Cancer Sci.* **2003**, *94*, 1029–1033.
- (7) Gu, H.; Neel, B. G. The “Gab” in signal transduction. *Trends Cell Biol.* **2003**, *13*, 122–30.
- (8) Deb, T. B.; Wong, L.; Salomon, D. S.; Zhou, G.; Dixon, J. E.; Gutkind, J. S.; Thompson, S. A.; Johnson, G. R. A common requirement for the catalytic activity and both SH2 domains of SHP-2 in mitogen-activated protein (MAP) kinase activation by the ErbB family of receptors. *J. Biol. Chem.* **1998**, *273*, 16643–16646.
- (9) Cunnick, J. M.; Dorsey, J. F.; Munoz-Antonia, T.; Mei, L.; Wu, J. Requirement of SHP-2 binding to Grb2-associated binder-1 for mitogen-activated protein kinase activation in response to lysophosphatidic acid and epidermal growth factor. *J. Biol. Chem.* **2000**, *275*, 13842–13848.
- (10) Maroun, C. R.; Naujokas, M. A.; Holgado-Madruga, M.; Wong, A. J.; Park, M. The tyrosine phosphatase SHP-2 is required for sustained activation of extracellular signal-regulated kinase and epithelial morphogenesis downstream from the met receptor tyrosine kinase. *Mol. Cell. Biol.* **2000**, *20*, 8513–8525.
- (11) Furge, K. A.; Zhang, Y. W.; Vande Woude, G. F. Met receptor tyrosine kinase: enhanced signaling through adapter proteins. *Oncogene* **2000**, *19*, 5582–5589.
- (12) Bentires-Alj, M.; Kontaridis, M. I.; Neel, B. G. Stops along the RAS pathway in human genetic disease. *Nat. Med.* **2006**, *12*, 283–285.
- (13) Higashi, H.; Tsutsumi, R.; Muto, S.; Sugiyama, T.; Azuma, T.; Asaka, M.; Hatakeyama, M. SHP-2 tyrosine phosphatase as an intracellular target of *Helicobacter pylori* CagA protein. *Science* **2002**, *295*, 683–686.
- (14) Meyer-ter-Vehn, T.; Covacci, A.; Kist, M.; Pahl, H. L. *Helicobacter pylori* activates mitogen-activated protein kinase cascades and induces expression of the proto-oncogenes c-fos and c-jun. *J. Biol. Chem.* **2000**, *275*, 16064–16072.

(15) Hof, P.; Pluskey, S.; Dhe-Paganon, S.; Eck, M. J.; Shoelson, S. E. Crystal structure of the tyrosine phosphatase SHP-2. *Cell* **1998**, *92*, 441–450.

(16) Shen, K.; Keng, Y. F.; Wu, L.; Guo, X. L.; Lawrence, D. S.; Zhang, Z. Y. Acquisition of a specific and potent PTP1B inhibitor from a novel combinatorial library and screening procedure. *J. Biol. Chem.* **2001**, *276*, 47311–47319.

(17) Huang, P.; Ramphal, J.; Wei, J.; Liang, C.; Jallal, B.; McMahon, G.; Tang, C. Structure-based design and discovery of novel inhibitors of protein tyrosine phosphatases. *Bioorg. Med. Chem.* **2003**, *11*, 1835–1849.

(18) Nören-Müller, A.; Reis-Correa, I.; Prinz, H.; Rosenbaum, C.; Saxena, K.; Schwalbe, H. J.; Vestweber, D.; Cagna, G.; Schunk, S.; Schwarz, O.; Schiewe, H.; Waldmann, H. Discovery of protein phosphatase inhibitor classes by biology-oriented synthesis. *Proc. Nat. Acad. Sci. U.S.A.* **2006**, *103*, 10606–10611.

(19) Chen, L.; Sung, S. S.; Yip, M. L. R.; Lawrence, H. R.; Ren, Y.; Guida, W. C.; Sefti, S. M.; Lawrence, N. J.; Wu, J. Discovery of a novel Shp2 protein tyrosine phosphatase inhibitor. *Mol. Pharmacol.* **2006**, *70*, 562–570.

(20) Neel, B. G.; Tonks, N. K. Protein tyrosine phosphatases in signal transduction. *Curr. Opin. Cell Biol.* **1997**, *9*, 193–204.

(21) Poole, A. W.; Jones, M. L. A SHPing tale: perspectives on the regulation of SHP-1 and SHP-2 tyrosine phosphatases by the C-terminal tail. *Cell. Signalling* **2005**, *17*, 1323–1332.

(22) Yang, J.; Liu, L.; He, D.; Song, X.; Liang, X.; Zhao, Z. J.; Zhou, G. W. Crystal structure of human protein-tyrosine phosphatase SHP-1. *J. Biol. Chem.* **2003**, *278*, 6516–6520.

(23) Tenev, T.; Keilhack, H.; Tomic, S.; Stoyanov, B.; Stein-Gerlach, M.; Lammers, R.; Krivtsov, A. V.; Ullrich, A.; Böhmer, F. D. Both SH2 domains are involved in interaction of SHP-1 with the epidermal growth factor receptor but cannot confer receptor-directed activity to SHP-1/SHP-2 chimera. *J. Biol. Chem.* **1997**, *272*, 5966–5973.

(24) O'Reilly, A. M.; Neel, B. G. Structural determinants of SHP-2 function and specificity in *Xenopus* mesoderm induction. *Mol. Cell. Biol.* **1998**, *18*, 161–177.

(25) Yang, J.; Liang, X.; Niu, T.; Meng, W.; Zhao, Z.; Zhou, G. W. Crystal structure of the catalytic domain of protein-tyrosine phosphatase SHP-1. *J. Biol. Chem.* **1998**, *273*, 28199–28207.

(26) The NCI Diversity set was obtained from the Developmental Therapeutics Program of the NCI/NIH. NSC refers to National Service Center. See the following: Milne, G. W. A.; Feldman, A.; Miller, J. A.; Daly, G. P.; Hammel, M. J. The NCI Drug Information System. 2. DIS pre-registry. *J. Chem. Inf. Comput. Sci.* **1986**, *26*, 159–168.

(27) Fong, T. A. T.; Shawver, L. K.; Sun, L.; Tang, C.; App, H.; Powell, T. J.; Kim, Y. H.; Schreck, R.; Wang, X.; Risau, W.; Ullrich, A.; Hirth, K. P.; McMahon, G. SU5416 is a potent and selective inhibitor of the vascular endothelial growth factor receptor (Flk-1/KDR) that inhibits tyrosine kinase catalysis, tumor vascularization, and growth of multiple tumor types. *Cancer Res.* **1999**, *59*, 99–106.

(28) Sun, L.; Tran, N.; Liang, C.; Tang, F.; Rice, A.; Schreck, R.; Waltz, K.; Shawver, L. K.; McMahon, G.; Tang, C. Design, synthesis, and evaluations of substituted 3-[3-(3- or 4-carboxyethyl)pyrrol-2-yl]methylenylindolin-2-ones as inhibitors of VEGF, FGF, and PDGF receptor tyrosine kinases. *J. Med. Chem.* **1999**, *42*, 5120–5130.

(29) Friesner, R. A.; Banks, J. L.; Murphy, R. B.; Halgren, T. A.; Klicic, J. J.; Mainz, D. T.; Repasky, M. P.; Knoll, E. H.; Shelley, M.; Perry, J. K.; Shaw, D. E.; Francis, P.; Shenkin, P. S. Glide: a new approach for rapid, accurate docking and scoring. 1. Method and assessment of docking accuracy. *J. Med. Chem.* **2004**, *47*, 1739–1749.

(30) Andersen, J. N.; Mortensen, O. H.; Peters, G. H.; Drake, P. G.; Iversen, L. F.; Olsen, O. H.; Jansen, P. G.; Andersen, H. S.; Tonks, N. K.; Möller, N. P. Structural and evolutionary relationships among protein tyrosine phosphatase domains. *Mol. Cell. Biol.* **2001**, *21*, 7117–7136.

(31) Lee, D.; Long, S. A.; Murray, J. H.; Adams, J. L.; Nuttall, M. E.; Nadeau, D. P.; Kikly, K.; Winkler, J. D.; Sung, C. M.; Ryan, M. D.; Levy, M. A.; Keller, P. M.; DeWolf, W. E., Jr. Potent and selective nonpeptide inhibitors of caspases 3 and 7. *J. Med. Chem.* **2001**, *44*, 2015–2026.

(32) Parrick, J.; Yahya, A.; Ijaz, A. S.; Yizun, J. Convenient preparation of 3,3-dibromo-1,3-dihydroindol-2-ones and indole-2,3-diones (isatins) from indoles. *J. Chem. Soc., Perkin Trans. 1* **1989**, 2009–2015.

(33) Bramson, H. N.; Corona, J.; Davis, S. T.; Dickerson, S. H.; Edelstein, M.; Frye, S. V.; Gampe, R. T., Jr.; Harris, P. A.; Hassell, A.; Holmes, W. D.; Hunter, R. N.; Lackey, K. E.; Lovejoy, B.; Luzzio, M. J.; Montana, V.; Rocque, W. J.; Rusnak, D.; Shewchuk, L.; Veal, J. M.; Walker, D. H.; Kuyper, L. F. Oxindole-based inhibitors of cyclin-dependent kinase 2 (CDK2): design, synthesis, enzymatic activities, and X-ray crystallographic analysis. *J. Med. Chem.* **2001**, *44*, 4339–4358.

(34) (a) Gee, K. R.; Sun, W.-C.; Bhalgat, M. K.; Upson, R. H.; Klaubert, D. H.; Latham, K. A.; Haugland, R. P. Fluorogenic substrates based on fluorinated umbelliferones for continuous assays of phosphatases and β -galactosidases. *Anal. Biochem.* **1999**, *273*, 41–48. (b) Montalibet, J.; Skorey, K. I.; Kennedy, B. P. Protein tyrosine phosphatase: enzymatic assays. *Methods* **2005**, *35*, 2–8.

(35) Chu, W.; Zhang, J.; Zeng, C.; Rothfuss, J.; Tu, Z.; Chu, Y.; Reichert, E., D.; Welch, J. M.; Mach, H. R. *N*-Benzylisatin sulfonamide analogues as potent caspase-3 inhibitors: synthesis, in vitro activity and molecular modeling studies. *J. Med. Chem.* **2005**, *48*, 7637–7647.

(36) Somasekhara, S.; Dighe, V. S.; Suthar, G. K.; Mukherjee, S. L. Chlorosulphonation of isatins. *Curr. Sci.* **1965**, *34*, 508.

JM8002526